Clim. Past Discuss., 7, 3653–3697, 2011
www.clim-past-discuss.net/7/3653/2011/
doi:10.5194/cpd-7-3653-2011

Climate of the Past Discussions

Climatic interpretation of the length fluctuations of Glacier Frías, North Patagonia, Argentina

P. W. Leclercq[1], P. Pitte[2], R. H. Giesen[1], M. H. Masiokas[2], and J. Oerlemans[1]

[1]IMAU, Utrecht University, Princetonplein 5, 3584 CC Utrecht, The Netherlands
[2]AINIGLIA, CCT Mendoza, Av Ruiz Leal s/n, 5500 Mendoza, Argentina

Received: 16 September 2011 – Accepted: 29 September 2011 – Published: 26 October 2011

Correspondence to: P. W. Leclercq (p.w.leclercq@uu.nl)

Published by Copernicus Publications on behalf of the European Geosciences Union.

Abstract

We explore the climatic information contained in the record of length fluctuations of Glaciar Frías, in the North Patagonian Andes of Argentina. This record is one of the longest and most detailed glacier records in southern South America, starting in 1639. In order to interpret the length variations of Glaciar Frías since the maximum Little Ice Age extent in 1639, we use a combination of a simplified surface energy-balance model to calculate the glacier mass balance, and a flow-line model to account for the dynamical response of the glacier to changes in the climatic forcing. The overall retreat of the glacier observed over 1639–2009 is best explained by an annual mean temperature increase of 1.16 °C or a decrease in annual precipitation of 34 %, most of which would have occurred during the 20th century. The glacier model is also forced with independent proxy-based reconstructions of precipitation and temperature, based on tree rings and a composition of documentary evidence, tree rings, sediments, corals, and ice cores. The uncertainties in the presently available proxy reconstructions are rather large, leading to a wide range in the modelled glacier length. Most of the observations lie within this range. However, in these reconstructions, the mid-17th century is too cold and the early 19th century ca. 0.7 °C too warm to explain the observed glacier lengths.

1 Introduction

To understand current climate variability and make reliable predictions of future climate change, knowledge of the past climate is needed. As instrumental measurement series have limited length, this requires the use of proxy-based information. This is especially the case in southern South America, where long instrumental records of good quality are scarce and mostly limited to lowland, populated areas in Chile and Argentina (Rosenblüth et al., 1997). Most of the available proxies in southern South America are based on dendrochronological records, where the climate-dependent rate

CPD
7, 3653–3697, 2011

of growth is measured from annual tree ring properties (e.g. ring width and density, see Boninsegna et al. (2009) for an overview). There are, however, other climate proxies. Exploiting as many independent sources as possible, increases the reliability of the resulting climate reconstructions. Recently, Neukom et al. (2010) and Neukom et al. (2011) have developed a gridded dataset of precipitation and temperature anomalies in southern South America, using a combination of different climate proxies. In addition to reconstructions based on Andean tree rings, they include a variety of other proxies, such as documentary evidence, ice-cores, and corals. However, the climatic information that can be derived from observed glacier length fluctuations in South America has not yet been fully exploited. So far, this information of glacier fluctuations in southern South America has only been used qualitatively (e.g. Harrison et al., 2007; Neukom et al., 2011).

Usually, the high-resolution, proxy-based climate reconstructions depend on transfer functions derived from correlations with observational data. One of the benefits of this approach is that the records allow for a proper statistical calibration and verification of the models used to develop the climate reconstructions. However, this type of reconstructions has various limitations inherent to the series available. For example, for tree-ring chronologies the capacity of capturing long-term (i.e. centennial scale) climate variability, is limited by the length of the original tree-ring series and by the process of standardisation intended to remove the biological trends in the records (Cook and Kairiukstis, 1990). Uncertainty in the validity of the transfer function over the entire period of reconstruction and the decrease of low frequency variability, lead to increasing uncertainties in the long term trends of reconstructed temperature and precipitation records (e.g. Briffa et al., 1998, 2001; Esper et al., 2002).

Information of glacier fluctuations can provide valuable complementary climatic information over the past centuries. Fluctuations in climate cause changes in the accumulation (snowfall) and ablation (melt) of a glacier, and thus affect the glacier mass budget. In turn, fluctuations in a glacier's mass budget lead to dynamical adjustment of the glacier geometry. The interaction between glaciers and climate is well understood, and

CPD
7, 3653–3697, 2011

can be described using physical relations (e.g. Oerlemans, 2001; Cook et al., 2003; Hock and Holmgren, 2005; Rye et al., 2010; Giesen and Oerlemans, 2010). Therefore, we are not dependent on empirical transfer functions when we use glacier fluctuations as a climate proxy. Despite the lower temporal resolution inherent to the response time of glaciers to climate change, past glacier fluctuations thus form a valuable climate proxy to complement existing temperature and precipitation reconstructions.

On centennial timescales, length fluctuations are generally the only known glacier variable. Combinations of documentary and geomorphological information has lead to high resolution glacier length records (e.g. Zumbühl and Holzhauser, 1988; Nussbaumer et al., 2011). However, the historical evidence available for the southern part of the Andes is far less extensive than for Europe. In this context, the length record of Glaciar Frías, in the Monte Tronador area in Northern Patagonia is a fairly detailed, long glacier length record (Villalba et al., 1990; Masiokas et al., 2009). In this study, we exploit this glacier length record by extracting information of the North Patagonian climate over the past four centuries.

Glacier length changes have been used previously to reconstruct large-scale temperature fluctuations, by analysing a large sample of glacier length records with a simple glacier model (Oerlemans, 2005; Leclercq and Oerlemans, 2011). This approach cannot be used for individual glaciers. The influence of precipitation variations cannot be neglected locally, and the simple model, although valid for the mean of a larger sample, is likely to perform poorly for an individual glacier. In order to study the response of Glaciar Frías to climatic changes during the last four centuries, we have modelled its dynamic response using a coupled glacier mass balance – ice dynamical model.

In the next section, we will describe the general setting of Glaciar Frías and the available information for driving and calibrating the glacier model. This model has two components: the first one calculating the surface mass balance from temperature and precipitation, and the second describing the ice-flow dynamics of the glacier. Section 3 gives a description of both components. In Sect. 4, we discuss the characteristics of Glaciar Frías derived from a steady-state run with modern climate. We then use the glacier model to extract the climatic information from the historic length record. First directly, by using dynamic calibration of the mass balance (Oerlemans, 1997a). Secondly, we force the glacier model with existing proxy climate records from this region. Comparing the resulting modelled glacier length with the observed glacier fluctuations gives an idea of the accuracy of the existing proxies. To conclude, we study the behaviour of Glaciar Frías under the projected climate change of the 21st century.

2 Data

2.1 Study site

Glaciar Frías (41.15° S, 71.83° W) is located on the north east face of Monte Tronador, a 3448 m high peak on the Chilean-Argentinean border in the North Patagonian Andes (Fig. 1). The climate of Glaciar Frías is temperate maritime, with prevailing westerlies and large amounts of precipitation, predominantly in winter (Villalba et al., 1990; Brock et al., 2007). The Patagonian Andes form an effective north-south barrier to the westerlies. Hence, the region is characterized by a large east-west precipitation gradient, with over 2 m of precipitation on the western side and less than 1 m on the eastern side (Villalba et al., 2003).

Monte Tronador has several glaciers on the Chilean as well as on the Argentinean side. These glaciers have shown a general pattern of recession since the Little Ice Age (LIA) maximum, identified in this area between the 17th and the 19th centuries (Villalba et al., 1990; Masiokas et al., 2010). Glaciar Casa Pangue has retreated 1938 m in the period 1911–2000 (WGMS, 2008 and earlier volumes) and the surface of its lower ablation area has thinned with $2.3 \pm 0.6\,\mathrm{m\,a^{-1}}$ on average between 1961 and 1998 (Bown and Rivera, 2007). Likewise, the regenerated portions of Glaciar Castaño Overo and the Glaciar Río Manso have retreated noticeably over the last decades (WGMS, 2008 and earlier volumes; Masiokas et al., 2010).

Glaciar Frías has also substantially retreated over the 20th century (Fig. 8). Between 1916 and 2009 the glacier terminus retreated 1.9 km. The fluctuations of Glaciar Frías have been reconstructed for the last four centuries from dendro-geomorphological, historical and field evidence (Villalba et al., 1990). The glacier flows into the Frías valley, and the historical position of the tongue was well below the tree line. This made it possible to reconstruct the length variations back to 1639, by dendrochronological dating of moraines (Villalba et al., 1990). In addition, there exist several historical sources since the mid-19th century, and field measurements from 1976 to 1985. For this study, the existing length record was revised and the length record has been extended using aerial photography and satellite images (Fig. 8, Table 1). At present, the length record of Glaciar Frías is the most detailed long record of South America (see Masiokas et al., 2009, for an overview of glacier length observations in South America). In addition, Frías glacier has no extensive debris cover, calving at the terminus, or surges. This makes the Frías glacier well suited for climate reconstruction, as it is free of glaciological processes that may complicate the interpretation of the length fluctuations in terms of climatic change.

Because of the diversity of methods used in the determination of the glacier length changes, the length record has a variety of uncertainties. The glacier outlines from satellite images and aerial photos have an exact date, and an uncertainty in derived glacier length is estimated to be 10–50 m, i.e. 2 pixels, to account for rectification and interpretation errors. The field measurements were carried out yearly at unspecified dates, and are considered to be accurate within 10 m. They are connected to the record with the frontal position in 1979 taken from a Corona satellite image. The dates of the historical sources are also well known, up to the year, but the spatial uncertainty can be large, especially for the 1856 etch (accuracy taken to be ±150 m). The positions of the dated moraines are well known (within 50 m) but the dating has an uncertainty in the determined age of the trees and in the estimated time of seedling establishment (Luckman, 2000). Villalba et al. (1990) give an uncertainty of 20 yr for the dating in the Frías valley.

CPD
7, 3653–3697, 2011

The geometry of Glaciar Frías has been derived from a 2009 SPOT 5 image (Table 1), in combination with the SRTM v.4 digital elevation model (DEM) from 2000. In 2009 glacier had an area of 6.54 km^2 and was 5.55 km long, flowing from the Argentinean summit of Monte Tronador at 3191 m down to 1450 m. The glacier surface is rather steep, with a mean slope of 0.32, but it has a more gentle slope around 2000 m (Fig. 2a). The glacier hypsometry is shown in Fig. 2b. A large part of the area is in the 2000–2200 m range, with a much narrower accumulation area above 2600 m. The present-day glacier tongue as well as the historical glacier tongue are also relatively narrow (Fig. 1).

In our dynamical model (Sect. 3.2) we use the central flowline and we parameterise the lateral glacier geometry with a trapezoidal cross section. The central flowline is determined from the DEM and corrected by visual inspection. The width of the valley floor and the slope of the valley walls are derived from 25 cross sections.

2.2 Meteorological and glacier mass balance data

Unfortunately, the amount of glaciological and meteorological information available for the Glaciar Frías area is scarce. No mass balance measurements are available for Tronador glaciers and meteorological records are either short, low resolution, or distant from the study site. Based on short term precipitation measurements made in the late 1950's, Gallopin (1978) estimated that annual precipitation in the accumulation area of Monte Tronador is between 4.5 and 7 m a^{-1}.

For two other glaciers in the Chilean Lake District, with a climate comparable to Glaciar Frías, glacier mass balances have been measured. Rivera et al. (2005) and Bown et al. (2007) describe glaciological mass balance measurements (stakes and snow density measurements) collected during the two hydrological years 2003/2004 and 2004/2005 on the southeastern glacier at Volcán Mocho-Choshuenco. This volcano is inactive since 1864 and lies 130 km north of Glaciar Frías (Fig. 1). The ELA of this glacier lies between 1950 and 2000 m. The winter balance at 2000 m varied between 2.9 and 4 m w.e. a^{-1}, and a large mass balance gradient of 0.015 m w.e. a^{-1} m^{-1}

CPD
7, 3653–3697, 2011

N Patagonian climate from modelling Glaciar Frías

P. W. Leclercq et al.

was measured. Brock et al. (2007) have operated an automatic weather station (AWS) during several periods in 2004 and 2005 on the Pichillancahue-Turbio glacier on the active Volcán Villarica, 190 km north of Glacier Frías (Fig. 1). Due to the volcanic activity of Volcán Villarica, the mass balance of this glacier is strongly influenced by tephra covering the surface. Therefore, these measurements of the surface energy balance are not directly applicable to the mass balance of Frías glacier. However, Brock et al. (2007) present several results of interest for this study: they measured significant melt events at the ELA during the accumulation season caused by high air temperatures, and they confirm the high accumulation and melt rates found by Rivera et al. (2005) and Bown et al. (2007). In a reconstruction of the ELA of glaciers along the Andes of South America from a compilation of 0 °C isotherm altitude and precipitation, Condom et al. (2007) give an ELA between 1800 and 2200 m for the region of Glaciar Frías. Carrasco et al. (2008) also give a similar value from improvements of the relations used by Condom et al. (2007) for the Southern Andes.

The meteorological stations nearest to Glaciar Frías with long, complete, temperature data are Bariloche at 55 km to the east and Puerto Montt at 100 km to the west (Fig. 1). At Puerto Montt, radio-sonde measurements are performed once or twice a day, but the record has a considerable amount of missing data. Long, complete precipitation measurements from sites close to the Glaciar Frías are also not available. The existing precipitation measurements show a very large precipitation gradient over the Andes (Villalba et al., 2003). The station of Punta Huano, located 35 km west of Glaciar Frías at 200 m altitude, has an average of 3.2 m a^{-1} over the 10 yr of precipitation measurements in the period 1969–1980, whereas at Bariloche, on the eastern side of the Andes, an average annual precipitation of 0.88 m is measured over the period 1931–2009.

Because of the lack of nearby weather stations with long and detailed records, we use ERA-interim reanalysis data (1 January 1989–18 December 2010; 0.75° resolution) (Simmons et al., 2006) to force the mass balance model. The ERA-interim data are extended with ERA-40 reanalysis data (ECMWF Re-Analysis, 1 September 1957–

CPD
7, 3653–3697, 2011

1 September 2002; 1.125° resolution) for the period 1 January 1980–31 December 1988. Although ERA-40 is available from 1957, data for the mid and high latitudes on the Southern Hemisphere are not reliable in the presatellite era (Bromwich and Fogt, 2004). The spatial resolution of the ERA reanalysis data is too low to adequately resolve the local weather on an individual mountain. Therefore, we are limited to a mass balance that is based on the climatology of the reanalysis. We calculate monthly averages of temperature at 2000 m, the lapse rate, and the amplitude of the daily cycle from the 6 hourly temperature values at the 4 grid points surrounding Glaciar Frías. The lapse rate and 2000 m temperature are derived from a linear fit through the pressure levels between 900 hPa and 500 hPa (10 levels for ERA-interim, 4 for ERA-40). The precipitation is calculated from the sum of convective and large-scale precipitation given at the surface-level. For each month of the year, the climatological averages over the 1980–2009 period are calculated for each grid point and bilinearly interpolated to the location of Glaciar Frías (Fig. 3).

The temperature climatologies at the four grid points are very similar, but the calculation of precipitation is more difficult. Because two of the four grid points used in the temperature calculation are located on the eastern side of the Andes, these give lower precipitation totals. As the glacier of our interest is on the water divide, where we expect the maximum precipitation, we only take the western grid points into account. Still, the ERA reanalysis precipitation of 2.05 m a^{-1} is much lower than is measured at Punta Huano station. This is probably due to the relatively low resolution of the ERA topography, as also the gradient in the ERA precipitation across the Andes is not as strong as derived from the measurements. For the input of the glacier mass balance model, described in the next section, we have increased the ERA precipitation with a factor 2.2, such that the modelled winter accumulation at 2000 m is in agreement with the measured winter accumulation of Mocho-Choshuenco. The relative distribution of the annual precipitation over the months in the ERA data is assumed to be correct.

2.3 Climate reconstructions for southern South America

For North Patagonia, several reconstructions of temperature (e.g. Villalba et al., 1997, 2003) and precipitation (e.g. Villalba et al., 1998; Lara et al., 2008; Boucher et al., 2011) exist. Neukom et al. (2010, 2011) have compiled a temperature and precipitation reconstruction for southern South America on a $0.5^\circ \times 0.5^\circ$ grid from a selection of the available proxy records. In this study, we use the Neukom et al. (2010, 2011) and the Villalba et al. (2003) reconstructions to drive the glacier model, and then examine how well the observed glacier lengths are reproduced.

Neukom et al. (2011) provide gridded summer (DJF) and winter (JJA) temperature anomalies at yearly resolution for the periods 900–1995 and 1706–1995, respectively. As with the ERA reanalysis data, we use the values of the four grid points surrounding Glaciar Frías to compute the temperature anomalies with bilinear interpolation. Since the mass balance of Frías is sensitive to temperature perturbations in every month of the year (see Sect. 4.1), we apply the summer anomaly not only to the three summer months DJF, but to the summer half year November–April. Likewise, the winter anomaly is applied to May–October. In the period before 1706, when no winter temperatures are available, we apply the summer anomaly to the entire year. Winter and summer precipitation anomalies (Neukom et al., 2010) are available for the period 1590–1995 and 1498–1995, respectively. Like with temperature, the precipitation anomalies of DJF are extended to the summer half year, and JJA precipitation anomalies to the winter half year, to get anomalies for every month of the year.

For additional comparison, we also drive the model with 1640–1987 tree-ring based annual temperature anomalies as reconstructed by Villalba et al. (2003) for the Monte Tronador region. The reconstructed temperature anomalies reflect the annual temperature anomalies (Villalba et al., 2003). These records are not used in the temperature reconstruction of Neukom et al. (2011); the two temperature reconstructions are independent. For precipitation we again use the Neukom et al. (2010) reconstruction. Annual average temperature anomalies of both reconstructions and precipitation anomalies are shown in Fig. 9c.

CPD
7, 3653–3697, 2011

3 Methods

3.1 Mass balance

The lack of mass balance and detailed meteorological measurements in the direct vicinity of Glaciar Frías makes it impossible to drive and validate a detailed surface energy balance model. In this study, a simple surface mass balance model is used to calculate the annual surface mass balance, following the approach of Oerlemans (2010), further extended in Giesen and Oerlemans (2011). The model is driven with monthly averaged temperatures and monthly precipitation totals of the ERA reanalysis (Sect. 2.2). A concise description of the model is given below, for details we refer to Giesen and Oerlemans (2011).

The annual surface mass balance at a certain point on the glacier is given by

$$B = \int_{\text{year}} P_{\text{snow}} + (1-r)\min\left(0; -\frac{Q}{\rho_{\text{w}} L_{\text{f}}}\right) \mathrm{d}t, \quad (1)$$

where P_{snow} (m w.e.) is the mass gained from solid precipitation and the mass loss is determined from the surface energy balance Q. Melt is assumed to occur when the surface energy balance is positive. Part r of the meltwater is allowed to refreeze in the snowpack. The constants ρ_{w} and L_{f} are the water density and latent heat of melt, respectively. The mass balance is calculated at hourly time steps.

Precipitation is assumed to increase linearly with altitude with lapse rate p (Table 2). Hourly precipitation is obtained by equally distributing the monthly total over all hourly timesteps of the month. Temperature is determined from the monthly mean temperatures and an additional daily cycle, with a monthly amplitude. Both the precipitation and the temperature lapse rate are constant throughout the year. Precipitation that falls at air temperatures below 1.5 °C is assumed to be solid P_{snow}.

Because humidity, cloudiness, and wind speed data are not available for the Frías glacier surface, the energy available for melt is calculated from a simplified representation of the surface energy balance that only requires temperature and solid precipitation

CPD
7, 3653–3697, 2011
N Patagonian climate from modelling Glaciar Frías
P. W. Leclercq et al.

as input. The surface energy is divided into the net solar radiative flux and a second term $\psi(T_a)$, that represents all other atmospheric fluxes as a function of air temperature only:

$$Q = (1-\alpha)\tau S_{in} + \psi. \tag{2}$$

The net incoming short-wave radiation is calculated by multiplying the incoming solar radiation at the top of the atmosphere on a plane with the mean slope and aspect of Glaciar Frías (S_{in}), with the (constant) atmospheric transmissivity τ (Table 2). S_{in} is calculated from standard astronomical relations (e.g. Iqbal, 1983). Subsequently, the part of the incoming solar radiation that is reflected by the surface with albedo α is subtracted. When no snow is present, we use a constant ice albedo α_{ice}. After fresh snow has fallen, α decreases exponentially in time, with a time-scale t^*, from the fresh snow albedo α_{frsnow} to the firn albedo α_{firn} (Oerlemans and Knap, 1998). For snowfall around the melting point, α_{frsnow} is dependent on air temperature. For small snow depths, α is a function of both the snow albedo and the ice albedo, according to a depth-scale d^* (Giesen and Oerlemans, 2010).

The remaining atmospheric fluxes (net long-wave radiation, latent and sensible heat) are parameterized by ψ as a function of air temperature only. The parameterization is based on in-situ measurements of these fluxes with automatic weather stations on several glaciers (Giesen and Oerlemans, 2011). A threshold temperature T_{thresh} is defined, below which ψ has the constant value ψ_{min} and above which ψ increases linearly with air temperature.

$$\psi = \begin{cases} \psi_{min} & \text{for } T_a < T_{thresh} \\ \psi_{min} + cT_a & \text{for } T_a \geq T_{thresh} \end{cases} \tag{3}$$

The best choice for the parameters T_{thresh}, c, and ψ_{min} depends on the climatic setting of the glacier. Here, the values that suit a wet climate, comparable to the maritime glaciers of Norway, are chosen. See Table 2 for the values of all model parameters.

CPD
7, 3653–3697, 2011

If snow is present, part of the meltwater that is formed when Q is positive is allowed to refreeze. Following Oerlemans (1991), this part r is dependent on the temperature of the subsurface layer T_{sub} (°C):

$$r = 1 - e^{T_{\text{sub}}}. \tag{4}$$

The refreezing of meltwater heats the snowpack, leading to a change in the subsurface temperature T_{sub}, calculated as

$$\frac{\mathrm{d}T_{\text{sub}}}{\mathrm{d}t} = \frac{rQ}{C}, \tag{5}$$

where C is the heat capacity of the subsurface layer, taken equivalent to a 2 m thick layer of ice. At the end of the ablation season (30 April), T_{sub} is reset to the annual mean air temperature. If this temperature is higher than 0 °C, T_{sub} is set to 0 °C, and no refreezing will occur. This means that for present-day climate refreezing occurs above 2350 m.

For the steady-state run with 1980–2009 climate, the mass balance model is run at 50 m intervals between 700 and 3400 m a.s.l. to calculate the climatic mass balance profile as a function of height. The dynamical model, described below, is forced with this profile, until a steady-state is reached. When the reconstructed monthly precipitation and temperature anomalies are used as input for the glacier mass-balance model, a mass-balance profile is calculated for each year in the period covered by the reconstruction (1600–1995 for Neukom et al., 2011 and 1640–1987 for Villalba et al., 2003), again from 50 m intervals between 700 and 3400 m. This mass balance record is then used to force the dynamical model for the same period, after a spin-up time of 100 yr with the mean mass balance profile of the first 30 yr of the reconstruction.

In order to infer climatic information directly from the historical length record of Glaciar Frías, the mass balance history is reconstructed by dynamic calibration (Oerlemans, 1997a). In this method, it is assumed that at all times the mass balance profile $B(z,t)$ can be described by an altitude-independent balance perturbation $\delta B(t)$ added to a reference profile $B_{\mathrm{ref}}(z)$:

$$B(z,t) = B_{\mathrm{ref}}(z) + \delta B(t) \tag{6}$$

The mass balance profile from the 1980–2009 climate is taken as the reference profile B_{ref}. The values for δB are taken such, that the difference between the modelled glacier length record and the observed glacier lengths is minimised. An optimised sequence of step functions is generally sufficient to describe δB. The model has a spin-up period of 100 yr with $\delta B_{\mathrm{start}}$, such that the glacier has the steady-state length of the first observation when the record starts. The dynamical glacier model is run for the period of the observed length record, forced by the reconstructed mass balance history. If the dynamical model reproduces the observed lengths, the mass balance history is assumed to be correct.

3.2 Glacier dynamics

We use a one-dimensional flowline model to describe the ice dynamics. This model has been used earlier in the study of several other glaciers (e.g. Stroeven et al., 1989; Greuell, 1992; Oerlemans, 1997a,b), so here we only give a brief description.

Starting from conservation of mass, we can define for each vertical cross sectional area S along the flowline:

$$\frac{\partial S}{\partial t} = \frac{\partial (US)}{\partial x} + wB, \tag{7}$$

where U is the vertical mean ice velocity of a cross section, w is the width at the glacier surface and B is the specific mass balance. We parameterise the cross section with a trapezoid. Thus, surface width w is given by:

$$w = w_0 + \lambda H, \tag{8}$$

where H is the glacier thickness and λ is the effective slope of the valley wall. The area of the cross section S is given by:

$$S = H(w_0 + \frac{1}{2}\lambda H). \tag{9}$$

Combining these three equations gives the time evolution of the ice thickness:

$$\frac{\partial H}{\partial t} = \frac{-1}{w_0 + \lambda H} \frac{\partial}{\partial x} \left\{ HU(w_0 + \frac{1}{2}\lambda H) \right\} + B. \tag{10}$$

We use the shallow ice approximation (SIA), such that the mean vertical ice velocity is entirely determined by the local driving stress σ (Budd et al., 1979). We separate the vertical mean ice velocity in a component due to sliding and a component due to ice deformation, given by:

$$U = U_d + U_s = f_\mathrm{d} H \sigma^3 + f_\mathrm{s} \frac{\sigma^3}{H}, \tag{11}$$

with σ given by the ice thickness H and surface slope $\frac{\partial h}{\partial x}$ (h is the surface altitude):

$$\sigma = -\rho g H \frac{\partial h}{\partial x}. \tag{12}$$

Substituting this expression for U into Eq. (10) gives the expression for the evolution of the ice thickness:

$$\frac{\partial H}{\partial t} = \frac{-1}{w_0 + \lambda H} \frac{\partial}{\partial x} \left\{ D \frac{\partial h}{\partial x} \right\} + B, \tag{13}$$

with D:

$$D = \left(w_0 + \frac{1}{2}\lambda H \right) \rho^3 g^3 H^3 \left\{ f_\mathrm{d} H^2 \left(\frac{\partial h}{\partial x} \right)^2 + f_\mathrm{s} \left(\frac{\partial h}{\partial x} \right)^2 \right\}. \tag{14}$$

CPD
7, 3653–3697, 2011

Equation (13) is solved on a staggered grid, with a grid size of 25 m. Time integration is done with a forward explicit scheme, in time steps of 0.00025 yr (approx. 2 h). The specific mass balance B is a function of surface altitude h and taken from the balance profile calculated with the mass balance model. For time-dependent simulations, B is recalculated every year.

The topography of the glacier bed of Glaciar Frías is unknown, except for that part of the valley that is currently deglaciated. The bed topography of the part that is currently covered by ice is derived from the model forced with the climatological mass balance (Sect. 3.1, Fig. 4). The bed altitude along the flow line and the glacier width at the bed are adjusted, following an iterative procedure, such that the modelled surface width and altitude in equilibrium state match the observed surface width and surface altitude along the flow line. The bed profile that reproduces the present-day surface best (Fig. 2a) has an overdeepening around $x = 3500$ m, followed by a bump that is at the same location as the ridge that is currently emerging from the ice at ca. 1800 m (Fig. 1).

4 Results and discussion

4.1 Steady state

Before using the coupled mass balance – glacier model for climate reconstruction, we examine the model's performance and sensitivities with a steady-state solution. The climatological conditions of the period 1980–2009 are used as input for the mass-balance model to calculate the present-day climatological mass balance profile (Fig. 4). The calculated profile is almost linear below the ELA at 2090 m, and the gradient becomes smaller for higher elevations. This is in line with mass balance profiles observed elsewhere (e.g. Andreassen et al., 2005). The calculated mass balance gradient of 0.0011 m w.e. m^{-1} a^{-1} is large, but smaller than measured at Mocho-Choshuenco. This could be caused by the less pronounced seasonality in the precipitation at the higher

CPD
7, 3653–3697, 2011

N Patagonian climate from modelling Glaciar Frías

P. W. Leclercq et al.

latitude of Glaciar Frías. The calculated ELA at Glaciar Frías is a bit higher than the ELA at the Mocho-Choshuenco. This is reasonable, as the Glaciar Frías flows to the north-east and thus receives more incoming short-wave radiation than the Mocho-Choshuenco, that flows towards the south-east. For a selected number of altitudes, the evolution of the cumulative mass balance throughout the hydrological year is shown in Fig. 5. The winter accumulation at 2000 m is 3.0 m w.e., but this all melts during the ablation season. The winter accumulation is in line with the accumulation at Mocho-Choshuenco. The annual precipitation at 2000 m that is needed for this amount of accumulation is 7.3 m w.e. a^{-1}, which is at the high end of the observations of Gallopin (1978). As shown by the mass balance at 2500 m, ablation is still substantial above the equilibrium line, but this is outpaced by the accumulation. The model shows that at 1000 m there is hardly any accumulation, so in the present-day climate the glacier tongue would sustain year-round melting when it reaches the bottom of the Frías valley.

If we force the ice-dynamical model with the calculated climatological mass balance of the period 1980–2009, the calculated equilibrium glacier length is 6025 m. This is in good agreement with the observed glacier lengths in this period (cf. Fig. 8, Table 1), indicating that the calculated mass balance is fairly accurate. The length of Frías glacier is very sensitive to small changes in the mass balance profile, due to the present-day geometry (the ELA is in the altitude range where the glacier has a large part of its area, while the terminus is narrow in the steep part, see Figs. 1, 2). However, because no measurements of the individual components of the energy budget are available, compensating errors can not be excluded.

In Fig. 6, the seasonal sensitivity characteristic (SSC) (Oerlemans and Reichert, 2000) of the mass balance of Glaciar Frías in equilibrium state is shown. The SSC consists of 24 numbers that give the sensitivity of the annual mass balance to monthly perturbations in precipitation and temperature. The temperature sensitivities indicate that Glaciar Frías is in a very maritime climate. The SSC values are large and the mass balance is sensitive to temperature changes in every month of the year. Even temperature anomalies in the winter season lead to a significant changes in the mass balance. Furthermore, variations in winter precipitation are more important for the mass balance than variations in summer precipitation. Most of the precipitation falls in winter, and summer precipitation falls as rain on a large part of the glacier.

To conclude we calculate the response time and climate sensitivity of the glacier in equilibrium state. This is done by imposing a stepwise perturbation in the climatic forcing that is kept constant until the glacier has reached a new equilibrium. The climate sensitivity indicates the difference between the two equilibria. The response time is a measure for the time needed to reach the new equilibrium, defined as the time needed to reach $(1-e^{-1})$ of the final change. As the mass balance is sensitive to temperature change in all months of the year, the perturbations consist of changes in the annual mean temperature, of -1.0, -0.5, 0.5 and 1.0 K. The resulting changes in glacier length and glacier volume are shown in Fig. 7. Frías has a response time of 14 a, for both volume and length changes. This is short compared with other alpine glaciers (cf. Jóhannesson et al., 1989; Greuell, 1992; Oerlemans, 1997a,b; Brugger, 2007; Laumann and Nesje, 2009), indicating that Glaciar Frías reacts rather directly to changes in climate. The climate sensitivity is dependent on the size of the perturbation, it varies between 1850–2950 m K^{-1} in terms of length change, and 0.22–0.38 $km^3\,K^{-1}$ in terms of volume change for the four perturbations used here. The large spread is caused by the strong dependence of the climate sensitivity on surface geometry and the bed topography at the glacier terminus. For limited perturbations, the terminus remains in the steep part between 5–7 km. For the temperature decrease of 1 K the terminus advances over the flat valley floor, whereas for a temperature increase of 1 K the glacier is forced to retreat into the overdeepening, which implies a major mass loss. For the limited perturbations of ±0.5 K, the climate sensitivity is 2700 m K^{-1} and 0.23 $km^3\,K^{-1}$.

CPD
7, 3653–3697, 2011

4.2 Historical fluctuations

4.2.1 Climatic information from dynamic calibration

As shown in Fig. 8, the observed length record can be reproduced very well using dynamic calibration of the mass balance profile with a sequence of 13 step functions. To explain the maximum glacier length in 1639, the mass balance profile must have been 1.5 m w.e. a^{-1} higher than the 1980–2009 mean profile. This maximum of δB is followed by a slight decline over the following two centuries, until the mass balance makes a significant drop at the end of the 19th century. In the 20th century, more length observations are available and thus the reconstructed δB then shows more fluctuations. The most striking fluctuation is around 1970, prior to the significant and well documented re-advance of the glacier, that culminated in 1977. Overall, there is a negative trend in the mass balance over the 20th century of -0.0077 m w.e. a^{-2}. The current retreat is best explained by $\delta B = -0.2$ m w.e. a^{-1} in the period 2001–2009. Hence, the glacier retreat over the entire period of the length record, 1639–2009, is best explained by a decrease in δB of 1.7 m w.e. a^{-1}.

Changes in the mass balance are in general due to changes in both precipitation and temperature. Although the influence of these two climate components can not be disentangled from the mass balance reconstruction, it is possible to give a quantitative indication of the change in temperature or precipitation needed to arrive at the reconstructed mass balance changes. The sensitivity of the mass balance profile to changes in annual temperature and precipitation is determined based on least squares fit of the mass balance profiles calculated with the temperature perturbations of ±0.5 and ±1 K and precipitation perturbations of ±10 and ±20 %. The mass balance sensitivity to changes in temperature is -1.46 m w.e. a^{-1} K^{-1}, and 0.51 m w.e. a^{-1} per 10 % increase in precipitation. The observed retreat of Glaciar Frías over the period 1639–2009 is thus best explained by a temperature increase of 1.16 K, or a precipitation decrease of 34 % (meaning that the precipitation in the 17th century must have been 134 % of

CPD
7, 3653–3697, 2011

present-day precipitation). Or, most likely, the observed glacier retreat is a combination of both.

Trenberth et al. (2007, Fig. 3.9) show a negative trend in measured surface temperature of −0.2 to −0.5 °C per century over the period 1901–2005 for the region of Tronador, in apparent contradiction to the decrease of the reconstructed mass balance. However, based on analyses of radiosonde data, Carrasco et al. (2008) conclude that the cooling in this region is restricted to the near-surface troposphere. At the 850 hPa level the temperature trend is positive for summer and winter (for 1958–2006: 0.013 and 0.014 K a^{-1}, respectively). In addition, Rivera et al. (2002) attribute the retreat of glaciers in Southern Chile for a large part to a decrease in precipitation. Indeed at Puerto Montt, precipitation has decreased by 20 % in the period 1958–2006. Simply adding these trends in precipitation and free atmosphere temperature gives a trend in δB of −0.03 m w.e. a^{-2} for 1958–2006. This is even larger than the trend in the reconstructed δB, which is −0.015 m w.e. a^{-2} over the same period.

4.2.2 Forcing the glacier model with climate reconstructions

Instead of deriving a mass balance reconstruction based on dynamical calibration, we can also calculate the historical mass balance using the temperature and precipitation records based on other proxy reconstructions. In this way the observed glacier length can serve as a constraint on the proxy-based climate reconstructions. This could in addition provide information on the relative contributions of fluctuations in precipitation and temperature to the glacier length changes. We force the glacier model with the reconstructions of Neukom et al. (2010, 2011) and Villalba et al. (2003). The calculated glacier length for the period 1600–1995 and 1640–1987, respectively, is shown together with the observed glacier length in Fig. 9a.

When we first focus on the results calculated from the Neukom et al. (2010, 2011) reconstructions, the modelled length is promising in a qualitative sense: maximum extents before 1800, in 1884 and in 1916 are reproduced (although the timing does not exactly match the dating of the moraines) together with the large retreat between

1880 and 1960, and the re-advance in the 70's that is followed by the retreat that continues up to present day. However, when the results are examined in more detail, the agreement is rather poor. The length variations in the 20th century are too large: the modelled glacier length in 1940 is 500 m larger than the observed length, while in 1970 it is 700 m shorter than observed, and the subsequent re-advance is again larger than observed. In the beginning of the 19th century the glacier is too small to reach the 1843 moraine, and the maximum extent in the 17th century is about 1 km too large. Only the 1727 and 1756 moraines are well reproduced.

We have also calculated the length record from perturbations in temperature only, leaving the precipitation constant at the 1980–2009 mean. The resulting length record closely resembles the length record of the model run with perturbations in both temperature and precipitation (Fig. 9a). This indicates that the fluctuations in precipitation are in general of minor importance for the observed glacier fluctuations over the last four centuries. The only significant difference between the two modelled length records is in the mid-17th century. In this period, a positive precipitation anomaly contributes to the glacier advance, accounting for an additional advance of 0.4 km (Fig. 9a, c).

The large fluctuations in the modelled length during the 20th century could be an indication that the modelled response of the glacier is too large. The length record could be smoother if the glacier response is reduced by changing the ice dynamics. However, adjusting the sliding and deformation velocities of the glacier with a different parameter choice for f_d and f_s (Eq. 11, Table 2) does not improve the modelled length record. Also the parameter choice in the mass balance model, where especially the parametrisation of ψ is uncertain, cannot explain the overestimated variations. Variation of these parameters lead to a more positive, or negative, mass balance for the entire period of reconstruction. Other parameter values thus lead to a constantly larger or smaller glacier, not to smaller or larger length fluctuations.

While the uncertainties in the glacier model cannot account for the discrepancies between the observed glacier length fluctuations and the modelled length from the climate reconstruction, the differences can to a large extent be explained by the uncertainties in the climate reconstructions. Using the decadal-scale uncertainties in the reconstructions of Neukom et al. (2010, 2011), we have estimated upper and lower limits for the modelled glacier length (dashed blue lines in Fig. 9a). For the upper limit we calculated maximum mass balance from the precipitation plus 1 SE uncertainty and the temperature minus the 1 SE uncertainty. Likewise, we calculated the lower limit in modelled glacier length from the minimal precipitation and maximal temperatures within the 1 SE uncertainty margin. The uncertainty in the reconstruction is fairly large, when translated into glacier length. Almost all glacier length observations fall within the range that is derived from uncertainty in the prescribed forcing. Only the constraints set by the maximum glacier length in the 1600–2009 period, as determined by the 1639 moraine, and the length measurements in 1843, 1936 and 1944 are not met. As the modelled maximum extent is reached in the period prior to 1706, when no winter temperature anomalies are available, this result should be interpreted with care. This is illustrated by the 900 m smaller extent when the summer anomaly prior to 1706 is only applied to the summer half of the year, keeping the winter temperatures at the 1980–2009 mean (dotted blue line in Fig. 9a). Furthermore, it is evident that the glacier is particularly sensitive to climatic forcing when the length is in the range of 5000–7000 m. When the terminus is in this range, the uncertainty band is much wider, without the uncertainties in precipitation or temperature being larger.

With the Villalba et al. (2003) reconstruction as temperature forcing, the modelled glacier length is comparable to the previous reconstruction (Fig. 9a). Again, the modelled length qualitatively shows the same characteristics as the observed record, but the reconstruction fails to reproduce the length observations on more or less the same points in time as the reconstruction forced with the Neukom et al. (2011) temperature anomalies. However, in this second reconstruction the maximum extent is smaller, more in line with the observations (but timed later). And, in contradiction to the other reconstruction, the glacier extent is much smaller than observed throughout the entire first half of the 20th century.

CPD
7, 3653–3697, 2011

We have calculated δB from the mass-balance profiles of both reconstructions (Fig. 9b), to compare the differences in mass balance profiles between the results of the dynamical calibration and those obtained when the model is forced with reconstructed temperature and precipitation anomalies from North Patagonia. As the calibrated mass-balance record only reproduces the observations in the simplest way, the mass-balance based on the reconstructed temperature and precipitation can not be expected to be identical. The glacier has likely experienced unobserved retreat in the periods between two maximum stands that are indicated by the moraines. With this in mind still three discrepancies between the observed and modelled glacier lengths can be identified: i) The δB based on Neukom et al. (2011) is more than 1 m w.e. a^{-1} too high in the period 1640–1660. ii) Both reconstruction-based δBs are too low to reproduce the observed length in 1843. An increase of 1 m w.e. a^{-1} in δB would reproduce the local maximum in glacier length, as indicated by the 1843 moraine. This modelled maximum is timed 15 yr before the dated age of the moraine, which is within the uncertainty range of the dating. iii) There is a striking difference between the two reconstruction-based mass balances in the first half of the 20th century. The Neukom et al. (2011) reconstruction results in a too high mass balance with a too large glacier extent, while the Villalba et al. (2003) gives a much lower δB, which results in a too small glacier extent during this period.

As the past glacier fluctuations appear to be mainly temperature driven, we express the differences in terms of temperature anomaly. It is difficult to draw firm conclusions for the period before 1706, as the uncertainties in the reconstructed mass balance are large due to the missing winter temperatures. If the summer anomaly is applicable to the winter anomaly, the best estimate of the reconstructed temperature of Neukom et al. (2011) for the middle of 17th century is in the order of 0.7–1.0 °C too low. The temperature reconstruction of Villalba et al. (2003) is compatible with the observed glacier length in this period, although the timing of the advance deviates from the dating of the moraine. Both reconstructions give too high temperatures around 1800. According to the modelled glacier length, the best estimate of the temperature anomaly should be

CPD
7, 3653–3697, 2011
N Patagonian climate from modelling Glaciar Frías
P. W. Leclercq et al.

0.7 °C lower in the period 1790–1820. The disagreement between the two reconstructions in the first half of the 20th century is remarkable, as for both reconstructions this period is part of the calibration period. The mass balance obtained from the dynamical calibration suggests that, for this period, the mean of the two temperature reconstructions would explain the observed glacier length.

These results arguably have a substantial uncertainty, which is difficult to quantify. The glacier mass balance model for this glacier is only validated with the steady-state length from reanalysis climatology. The reliability of the model would greatly improve from mass-balance measurements at the Glaciar Frías. Local weather observations on the Glaciar Frías could help to determine the uncertainty that originates from using coarse resolution meteorological and climatological information as input (Hofer et al., 2010). Furthermore, the glacier is shown to be sensitive to temperature variations throughout the entire year, while in the case of Neukom et al. (2010, 2011) only values for the summer and winter months are given. Still, in view of the uncertainties associated with the climate reconstructions used in this study, the additional climatic information provided by glacier length fluctuations can be of great value. The modelled glacier length gives an extra constraint within the relatively large uncertainty range of the climate reconstructions, and in addition suggests to adjust the decadal average of certain periods in the reconstructions.

4.3 Future of Glaciar Frías

Regional climate projections for South America predict a warming trend and decrease in precipitation over the next century for North Patagonia (Vera et al., 2006; Christensen et al., 2007). According to the A1B scenario, by the end of the 21st century the annual precipitation will have decreased by 15 %, compared to the 1980–1999 average. Winter (JJA) precipitation will decrease by 5–10 %, while the projected summer (DJF) precipitation loss is predicted to go up to 30 %. For the period 2080–2099, annual mean temperature is projected to be 2 °C higher than in the reference period 1980–1999, with the changes in summer temperature (+2.5 °C) being stronger than in winter (+1.5 °C).

CPD
7, 3653–3697, 2011

Figure 10 shows the future response of Glaciar Frías to the projected changes in North Patagonian climate. For simplicity, the coupled model was forced with a linear increase in annual temperature and a linear decrease in annual precipitation, such that in 2100 the annual temperature is 2 °C higher than the 1980–2009 average, and annual precipitation has decreased with 10 % in 2100 (in the annual mean we have given the projected change in winter precipitation more weight than the change in summer precipitation, as the mass balance is hardly sensitive to summer precipitation, cf. Fig. 6). Based on this scenario, the projected retreat of Glaciar Frías is quite dramatic. Under the conditions of a 2 °C temperature rise and a 10 % decrease in annual precipitation, the glacier will retreat 3400 m to a length of 2175 m in 2100. This projected retreat in length is larger than the retreat since the maximum stand in 1639. The terminus will retreat to an elevation of 2150 m, while it currently is at 1450 m. In terms of volume, the shrinkage is even more pronounced: the glacier is projected to loose more than 80 % of its volume during the 21st century. A simple sensitivity test, in which the precipitation is kept at the 1980–2009 level (dashed black in Fig. 10), shows that the glacier retreat is mainly due to the increase in temperature. The extra precipitation slows down the retreat, but the eventual mass loss is very similar.

5 Conclusions

In this study we have presented a model for Glaciar Frías in the North Patagonian Andes of Argentina. This glacier, which has the most detailed, long record of LIA and post-LIA fluctuations in southern South America (currently spanning the period 1639–2009), has a land-based tongue, and is free from extensive debris cover. Therefore, Glaciar Frías is well suited for the study of past climate of the Northern Patagonian Andes. Given the lack of detailed meteorological information near Glaciar Frías, we forced a simplified surface-energy balance model with climatological monthly temperature and precipitation values derived from ERA reanalysis. The results provided interesting new information regarding the climate sensitivity of this glacier and offered for the first time in Patagonia the possibility of comparing modelled glacier mass balance changes with those obtained from independent, proxy-based climate reconstructions.

Glaciar Frías is located in a temperate maritime climate. It is very sensitive temperature changes throughout the entire mass-balance year, with a stronger sensitivity to changes in summer than to changes in winter temperature. The mass balance is to a lesser extent sensitive to variations in precipitation, mainly to changes in winter precipitation. Glaciar Frías has a response time of only 14 a, and therefore follows fluctuations in climate quite closely. The calculated present-day mass balance corresponds well with the little information that is available in the North Patagonian Andes. Moreover, the equilibrium length with present-day climate (6025 m) is within the range expected from the glacier length observations. This indicates that the model is performing well and gives confidence in the deduced sensitivity of the glacier to changes in regional climate.

The reconstructed mass balance history indicates that the overall retreat of Glaciar Frías during the period 1639–2009 can be best explained by a decrease of 1.7 m w.e. a^{-1} of the specific mass balance profile. This change in climatic conditions can be caused by an increase in temperature as well as, or in combination with, a decrease in precipitation. If it would only be attributed to changing precipitation, the precipitation in the mid-17th century must have been 134 % of the 1980–2009 average. If attributed to temperature, the mass balance decrease implies a temperature increase of 1.16 °C. Until the mid of the 19th century, North Patagonian climate was in a relatively stable state, with only minor warming/drying. At the end of the 19th century, mass balance dropped substantially and continued to decrease until the 21st century, with some fluctuations of which the most striking was around 1970.

Driving the glacier model with independently reconstructed temperature and precipitation shows that the fluctuations of Glaciar Frías over the last four centuries were predominantly temperature-driven. Glacier length records can, in combination with a glacier model, also be used to validate or constrain high resolution proxies. In the case of North Patagonia, existing proxy-based reconstructions of precipitation and

CPD
7, 3653–3697, 2011

temperature seem to reconstruct the interdecadal variability well. The glacier model forced with these reconstructions produces glacier advances and retreats that in timing agree well with the dated moraines and observations. However, in quantitative sense, the reconstructed anomalies have a relatively high level of uncertainty. This is reflected in the large range of possible glacier lengths. In addition, to explain the observed glacier lengths of Glaciar Frías, temperature around 1800 must have been 0.7 °C lower than the best estimate of the reconstructed temperatures by Neukom et al. (2011) and Villalba et al. (2003), and up to 1 °C higher around 1640 than reconstructed by Neukom et al. (2011). Error margins in these results might be substantial, due to uncertainties in the climate reconstructions and in the glacier model, but are difficult to quantify. The uncertainties in the glacier model could substantially be reduced by performing mass-balance measurements and weather observations on Glaciar Frías.

Following the IPCC A1B scenario for North Patagonia, Glaciar Frías is projected to continue its rapid retreat in the near future. By 2100, the glacier will likely have lost more than 80 % of its present-day volume and the terminus will have retreated high up the Monte Tronador. Like with the past fluctuations, this expected retreat is mostly due to the projected increase in temperature.

Acknowledgements. We thank R. Neukom and R. Villalba for kindly providing their climate reconstructions, E. Betman for processing the Puerto Montt radio sonde data, and W. J. van den Berg for his help with the analysis of the ERA-reanalysis data. This study is supported by the Netherlands Organisation for Scientific Research (NWO), research program 816.01.016.

References

Agostini, A.: Nahuel-Huapí – Bellezas Naturales de los Andes en la Patagonia Septentrional, Agostini: Estudios Fotográficos, Buenos Aires, Argentina, 1949. 3685

Andreassen, L. M., Elvehøy, H., Kjøllmoen, B., Engeset, R. V., and Haakensen, N.: Glacier mass-balance and length variation in Norway, Ann. Glaciol., 42, 317–325, 2005. 3668

Boninsegna, J. A., Argollo, J., Aravena, J. C., Barichivich, J., Christie, D., Ferrero, M. E., Lara, A., Le Quesne, C., Luckman, B. H., Masiokas, M., Morales, M., Oliveira, J. M., Roig, F.,

Srur, A., and Villalba, R.: Dendroclimatological reconstructions in South America: a review, Palaeogeogr. Palaeoclim. Palaeoecol., 281, 210–228, doi:10.1016/j.palaeo.2009.07.020, 2009. 3655
Boucher, E., Guiot, J., and Chapron, E.: A millennial multi-proxy reconstruction of summer PDSI for southern South America, Clim. Past, 7, 957–974, doi:10.5194/cp-7-957-2011, 2011. 3662
Bown, F. and Rivera, A.: Climate changes and recent glacier behaviour in the Chilean Lake District, Global Planet. Change, 59, 76–86, 2007. 3657
Bown, F., Rivera, A., Acuña, C., and Casassa, G.: Recent glacier mass balance calculations at Volcán Mocho-Choshuenco (40° S), Chilean Lake District, vol. 318, IAHS Publ. Wallingford, UK, 143–152, 2007. 3659, 3660
Briffa, K. R., Schweingruber, F. H., Jones, P. D., Osborn, T. J., Shiyatov, S. G., and Vaganov, E. A.: Reduced sensitivity of recent tree-growth to temperature at high northern latitudes, Nature, 391, 678–682, 1998. 3655
Briffa, K. R., Osborn, T. J., Schweingruber, F. H., Harris, I. C., Jones, P. D., Shiyatov, S. G., and Vaganov, E. A.: Low-frequency temperature variations from a northern tree ring density network, J. Geophys. Res., 106, D3, 2001. 3655
Brock, B., Rivera, A., Casassa, G., Bown, F., and Acuña, C.: The surface energy balance model of an active ice-covered volcano: Villarrica Volcano, Southern Chile, Ann. Glaciol., 45, 104–114, 2007. 3657, 3660
Bromwich, D. H. and Fogt, R. L.: Strong trends in the skill of the ERA-40 and NCEP-NCAR reanalyses in the high and midlatitudes of the Southern Hemisphere, 1958–2001, J. Climate, 17, 4603–4619, 2004. 3661
Brugger, K. A.: The non-synchronous response of Rabots Glaciär and Storglaciären, Northern Sweden, to recent climate change: a comparative study, Ann. Glaciol., 46, 275–282, 2007. 3670
Carrasco, J. F., Osorio, R., and Casassa, G.: Secular trend of the equilibrium-line altitude on the western side of the southern Andes, derived from radiosonde and surface observations, J. Glaciol., 54, 538, 2008. 3660, 3672
Christensen, J. H., Hewitson, B., Busuioc, A., Chen, A., Gao, X., Held, I., Jones, R., Kolli, R. K., Kwon, W.-T., Laprise, R., Magaña Rueda, V., Mearns, L., Menéndez, C. G., Räisänen, J., Rinke, A., Sarr, A., and Whetton, P.: Regional climate projections, in: Climate Change 2007: The Physical Science Basis. Contribution of Working Group I to the fourth Assessment Report of the Intergovernmental Panel on Climate Change, edited by: Solomon, S., Qin, D.,

Manning, M., Chen, Z., Marquis, M., Averyt, K. B., Tignor, M., and Miller, H. L., Camebridge University Press, Camebridge, UK and New York, NY, USA, 2007. 3676

Condom, T., Coudrain, A., Sicart, J. E., and Théry, S.: Computation of the space and time evolution of equilibrium-line altitudes on Andean glaciers (10° N–55° S), Global Planet. Change, 59, 189–202, 2007. 3660

Cook, E. R. and Kairiukstis, L. A. (Eds.): Methods of dendrochronology, applications in the environmental sciences, Kluwer Academic Publishers, Dordrecht, The Netherlands, 1990. 3655

Cook, K. H., Yang, X., Carter, C. M., and Belcher, B. N.: A modeling system for studying climate controls on mountains glaciers with application to the Patagonian Icefields, Climatic Change, 56, 339–367, 2003. 3656

Esper, J., Cook, E. R., and Schweingruber, F. H.: Low-frequency signals in long tree-ring chronologies for reconstructing past temperature variability, Science, 295, 2250–2253, 2002. 3655

Fonk, F.: Diario del Fray Fransisco Menéndez a la Cordillera, Colección Biblioteca National, Valparaiso, Chile, 1886. 3685

Gallopin, G. C.: Estudio Ecológico integrado de la cuenca del Río Manso Superior, (Río Negro, Argentina). Part I. Descripción general de la cuenca, in: Anales de Parques Nacionales, vol. XIV, Servicio Nacional de Parques Nacionales, Buenos Aires, Argentina, 161–230, 1978. 3659, 3669

Giesen, R. H. and Oerlemans, J.: Response of the ice cap Hardangerjøkulen in Southern Norway to the 20th and 21st century climates, The Cryosphere, 4, 191–213, doi:10.5194/tc-4-191-2010, 2010. 3656, 3664

Giesen, R. H. and Oerlemans, J.: A simple surface mass balance model, in preparation, 2011. 3663, 3664

Greuell, W.: Hintereisferner, Austria: mass-balance reconstruction and numerical modelling of the historical length variations, J. Glaciol., 38, 233–244, 1992. 3666, 3670

Harrison, S., Winchester, V., and Glasser, N.: The timing and nature of recession of outlet glaciers of Hielo Patagonico Norte, Chile, from their Neoglacial IV (Little Ice Age) maximum positions, Global Planet. Change, 59, 67–78, doi:10.1016/j.gloplacha.2006.11.020, 2007. 3655

Hock, R. and Holmgren, B.: A distributed surface energy-balance model for complex topography and its application to Störglaciären, Sweden, J. Glaciol., 51, 25–36, 2005. 3656

Hofer, M., Mölg, T., Marzeion, B., and Kaser, G.: Empirical-statistical downscaling of reanalysis data to high-resolution air temperature and specific humidity above a glacier surface (Cordillera Blance, Peru), J. Geophys. Res., 115, D12120, doi:10.1029/2009JD012556, 2010. 3676

Iqbal, M.: An Introduction to Solar Radiation, Academic Press, New York – London, 1983. 3664

Jóhannesson, T., Raymond, C., and Waddington, E.: Time-scale for adjustment of glaciers to changes in mass balance, J. Glaciol., 35, 355–369, 1989. 3670

Lara, A., Villalba, R., and Urrutia, R.: A 400-year tree-ring record of the Puelo River summer-fall streamflow in the Valdivian Rainforest eco-region, Chile, Climatic Change, 86, 331–356, doi:10.1007/s10584-007-9287-7, 2008. 3662

Laumann, T. and Nesje, A.: The impact of climate change on future frontal variations of Brikdalsbreen, Western Norway, J. Glaciol., 55, 789–796, 2009. 3670

Leclercq, P. W. and Oerlemans, J.: Global and hemispheric temperature reconstruction from glacier length fluctuations, Clim. Dynam., online first, doi:10.1007/s00382-011-1145-7, 2011. 3656

Luckman, B. H.: The Little Ice Age in the Canadian Rockies, Geomorphology, 32, 357–384, doi:10.1016/S0169-555X(99)00104-X, 2000. 3658

Masiokas, M. H., Rivera, A., Espizúa, L. E., Villalba, R., Delgado, S., and Aravena, J. C.: Glacier fluctuations in extratropical South America during the past 1000 yr, Palaeogeogr. Palaeoclim. Palaeoecol., 281, 242–268, doi:10.1016/j.palaeo.2009.08.006, 2009. 3656, 3658

Masiokas, M. H., Luckman, B. H., Villalba, R., Ripalta, A., and Rabassa, J.: Little Ice Age fluctuations of Glaciar Río Manso in the North Patagonian Andes of Argentina, Quaternary Res., 73, 96–106, doi:10.1016/j.yqres.2009.08.004, 2010. 3657

Neukom, R., Luterbacher, J., Villalba, R., Küttel, M., Frank, D., Jones, P. D., Grosjean, M., Esper, J., Lopez, L., and Wanner, H.: Multi-centennial summer and winter precipitation variability in Southern South America, Geophys. Res. Lett., 37, L14708, doi:10.1029/2010GL043680, 2010. 3655, 3662, 3672, 3674, 3676, 3696

Neukom, R., Luterbacher, J., Villalba, R., Küttel, M., Frank, D., Jones, P. D., Grosjean, M., Wanner, H., Aravena, J. C., Black, D. E., Christie, D. A., D'Arrigo, R., Lara, A., Morales, M., Soliz-Camboa, C., Srur, S., Urrutia, R., and von Gunten, L.: Multiproxy summer and winter surface air temperature field reconstructions for Southern South America covering the past centuries, Clim. Dynam., 37, 35–51, doi:10.1007/s00382-010-0793-3, 2011. 3655, 3662, 3665, 3672, 3674, 3675, 3676, 3679, 3696

Nussbaumer, S. U., Nesje, A., and Zumbühl, H. J.: Historical glacier fluctuations of Jostedalsbreen and Folgefonna (Southern Norway) reassessed by new pictorial and written evidence, The Holocene, 21, 455–471, doi:10.1177/095968361, 2011. 3656

Oerlemans, J.: The mass balance of the Greenland ice sheet: sensitivity to climate change as revealed by energy-balance modelling, The Holocene, 1, 40–48, 1991. 3665

Oerlemans, J.: A flow-line model for Nigardsbreen: projection of future glacier length based on dynamic calibration with the historic record, Ann. Glaciol., 24, 382–389, 1997a. 3657, 3665, 3666, 3670

Oerlemans, J.: Climate sensitivity of Franz Josef Glacier, New Zealand, as revealed by numerical modelling, Arctic Alpine Res., 29, 233–239, 1997b. 3666, 3670

Oerlemans, J.: Glaciers and Climate Change, AA Balkema Publishers, Rotterdam, The Netherlands, 2001. 3656

Oerlemans, J.: Extracting a climate signal from 169 glacier records, Science, 308, 675–677, 2005. 3656

Oerlemans, J.: The microclimate of valley glaciers, Igitur, Utrecht Publishing & Archiving Services, Universiteitsbibliotheek Utrecht, Utrecht, The Netherlands, 2010. 3663

Oerlemans, J. and Knap, W. H.: A 1 yr record of global radiation and albedo in the ablation zone of Morteratschgletscher, Switserland, J. Glaciol., 44, 231–238, 1998. 3664

Oerlemans, J. and Reichert, B. K.: Relating glacier mass balance to meteorological data using a Seasonal Sensitivity Characteristic (SSC), J. Glaciol., 46, 1–6, 2000. 3669

Rivera, A., Acuña, C., Casassa, G., and Bown, F.: Use of remotely sensed and field data to estimate the contribution of Chilean glaciers to eustatic sea-level rise, Ann. Glaciol., 34, 367–372, 2002. 3672

Rivera, A., Bown, F., Casassa, G., Acuña, C., and Clavero, J.: Glacier shrinkage and negative mass balance in the Chilean Lake District (40° S), Hydrolog. Sci. J., 50, 2005. 3659, 3660

Rosenblüth, B., Fuenzaliba, H. A., and Aceituno, P.: Recent temperature variations in southern South America, Int. J. Climatol., 17, 67–85, 1997. 3654

Rye, C. J., Arnold, N. S., Willis, I. C., and Kohler, J.: Modeling the surface mass balance of high Arctic glacier using the ERA-40 reanalysis, J. Geophys. Res., 115, F02014, doi:10.1029/2009JF001364, 2010. 3656

Simmons, A., Uppala, S., Dee, D., and Kobayashi, S.: ERA-Interim: new ECMWF reanalysis products from 1989 onwards, ECMWF Newsletter, 110, 25–35, 2006. 3660

Stroeven, A., Van de Wal, R., and Oerlemans, J.: Historic front variations of the Rhone Glacier:

simulation with an ice flow model, in: Glacier Fluctuations and Climate Change, edited by: Oerlemans, J., Glaciology and quaternary geology, Kluwer Academic Publishers, Dordrecht, The Netherlands, 1989. 3666

Trenberth, K. E., Jones, P. D., Ambenje, P., Bojariu, R., Easterling, D., Tank, A. K., Parker, D., Rahimzadeh, F., Renwick, J. A., Rusticucci, M., Soden, B., and Zhai, P.: Climate change 2007: The physical science basis. Contribution of working groups I to the fourth assessment report of the Intergovernmental Panel on Climate Change, chap. 3, Cambridge University Press, Cambridge, UK and New York, NY, USA, 2007. 3672

Vera, C., Silvestri, G., Liebmann, B., and González, P.: Climate change scenarios for seasonal precipitation in South America from IPCC-AR4 models, Geophys. Res. Lett., 33, L13707, doi:10.1029/2006GL025759, 2006. 3676

Villalba, R., Leiva, J. C., Rubulls, S., Suarez, J., and Lenzano, L.: Climate, tree-ring and glacial fluctuations in the Rio Frias Valley, Rio Negro, Argentina, Arctic Alpine Res., 22, 215–232, 1990. 3656, 3657, 3658, 3685

Villalba, R., Boninsegna, J. A., Veblen, T. T., Schmelter, A., and Rubulis, S.: Recent trends in tree-ring records from high elevation sites in the Andes of Northern Patagonia, Climatic Change, 36, 425–454, 1997. 3662

Villalba, R., Cook, E. R., Jacoby, G. C., D'Arrigo, R. D., Veblen, T. T., and Jones, P. D.: Tree-ring based reconstructions of Northern Patagonia precipitation since AD 1600, The Holocene, 8, 659–674, doi:10.1191/095968398669095576, 1998. 3662

Villalba, R., Lara, A., Boninsegna, J. A., Masiokas, M. H., Delgado, S., Aravena, J. C., Roig, F. A., Schmelter, A., Wolodarsky, A., and Ripalta, A.: Large-scale temperature changes across the Southern Andes: 20th-century variations in the context of the past 400 yr, Climatic Change, 59, 177–232, 2003. 3657, 3660, 3662, 3665, 3672, 3674, 3675, 3679, 3696

WGMS: Fluctuations of Glaciers, vol. I–IX, ICSU (FAGS)/IUGG (IACS)/UNEP/UNESCO/WMO, World Glacier Monitoring Service, Zurich, Switzerland, 2008 and earlier volumes. 3657

Zumbühl, H. J. and Holzhauser, H.: Alpengletscher in der Kleinen Eiszeit, *Die Alpen*, vol. 3, Schweizerischen Alpen Club, Bern, Switzerland, 1988. 3656

CPD
7, 3653–3697, 2011

N Patagonian climate from modelling Glaciar Frías

P. W. Leclercq et al.

Table 1. Glacier length record of Glaciar Frías used in this study, including year of measurement (or reconstructed date of maximum extent), total length along the flowline (km), cumulative length change (m), method of observation (*moraine* indicates a moraine dated with dendrochronology, *historical* are historical sketches and photos, *field* denotes field measurements of terminus position, and *Landsat*, *Corona*, *SPOT* and *ASTER* are positions measured from satellite images), data source, and estimate of accuracy of the length measurement (m).

year	L (km)	dL (m)	type	source	accuracy (m)
1639	7.90	0	moraine	Villalba et al. (1990)	50
1727	7.63	−262	moraine	Villalba et al. (1990)	50
1752	7.58	−316	moraine	Villalba et al. (1990)	50
1843	7.53	−364	moraine	Villalba et al. (1990)	50
1856	7.50	−400	historical	Fonk (1886)	150
1884	7.35	−549	moraine	Villalba et al. (1990)	50
1916	7.14	−752	moraine	Villalba et al. (1990)	50
1936	6.77	−1125	historical	Agostini (1949)	20
1944	6.77	−1125	aerial	SHN	10
1970	6.36	−1534	aerial	IGM	10
1973	6.74	−1157	Landsat MSS	GLCF	120
1976	6.78	−1141	field	S. Rubulis	10
1977	6.77	−1121	field	S. Rubulis	10
1978	6.74	−1159	field	S. Rubulis	10
1979	6.71	−1181	field/Corona	S. Rubulis/EROS	10
1980	6.69	−1207	field	S. Rubulis	10
1981	6.61	−1231	field	S. Rubulis	10
1982	6.62	−1277	field	S. Rubulis	10
1983	6.55	−1343	field	S. Rubulis	10
1984	6.47	−1427	field	S. Rubulis	10
1985	6.44	−1453	field	S. Rubulis	10
1986	6.32	−1463	Landsat TM	GLCF	50
1987	6.29	−1495	Landsat TM	GLCF	50
1996	5.89	−1886	field	S. Rubulis	20
2003	5.56	−2607	ASTER	GLIMS	30
2007	5.73	−2444	Landsat ETM	CONAE	50
2009	5.55	−2617	SPOT	Spot image	10

SHN	Servicio de Hidrografía Naval, Argentina
IGM	Instituto Geográfico Nacional, Argentina
GLCF	Global Land Cover Facility, University of Maryland, US
S. Rubulis	field measurements of S. Rubulis, reported in Villalba et al. (1990)
EROS	Earth Resources Observation and Science Center, US Geological Survey
GLIMS	Global Land Ice Measurements from Space
CONAE	Comisión Nacional de Actividades Espaciales, Argentina

CPD
7, 3653–3697, 2011

N Patagonian climate from modelling Glaciar Frías

P. W. Leclercq et al.

Table 2. Model parameter values of the surface mass balance model and the ice-dynamical model.

Parameter	Symbol	Value	Unit
Temperature lapse rate	γ	0.0048	$\mathrm{K\,m^{-1}}$
Precipitation vertical gradient	p	0.0015	$\mathrm{m\,a^{-1}\,m^{-1}}$
Threshold temperature for snow	T_{snow}	1.5	$^{\circ}\mathrm{C}$
Atmospheric transmissivity	τ	0.5	
Water density	ρ_{w}	1000	$\mathrm{kg\,m^{-3}}$
Ice density	ρ_{ice}	900	$\mathrm{kg\,m^{-3}}$
Latent heat of melt	L_{f}	$3.34\ 10^{5}$	$\mathrm{J\,kg^{-1}}$
Fresh snow albedo	α_{frsnow}	0.69–0.90	
Firn albedo	α_{firn}	0.53	
Ice albedo	α_{ice}	0.35	
Albedo time-scale	t^{*}	21.9	days
Albedo depth-scale	d^{*}	0.001	m w.e.
Heat capacity of subsurface layer	C	$3.76\ 10^{6}$	$\mathrm{J\,m^{-2}\,K^{-1}}$
Threshold temperature $\psi(T_{\mathrm{a}})$	T_{thresh}	0.44	$^{\circ}\mathrm{C}$
Minimum $\psi(T_{\mathrm{a}})$	ψ_{min}	–30	$\mathrm{W\,m^{-2}}$
Slope $\psi(T_{\mathrm{a}})$	c_1	9	$\mathrm{W\,m^{-2}\,K^{-1}}$
Sliding constant	f_{s}	$5.7\ 10^{-20}$	$\mathrm{Pa^{-3}\,m^{2}\,s^{-1}}$
Deformation constant	f_{d}	$1.9\ 10^{-24}$	$\mathrm{Pa^{-3}\,s^{-1}}$

CPD
7, 3653–3697, 2011

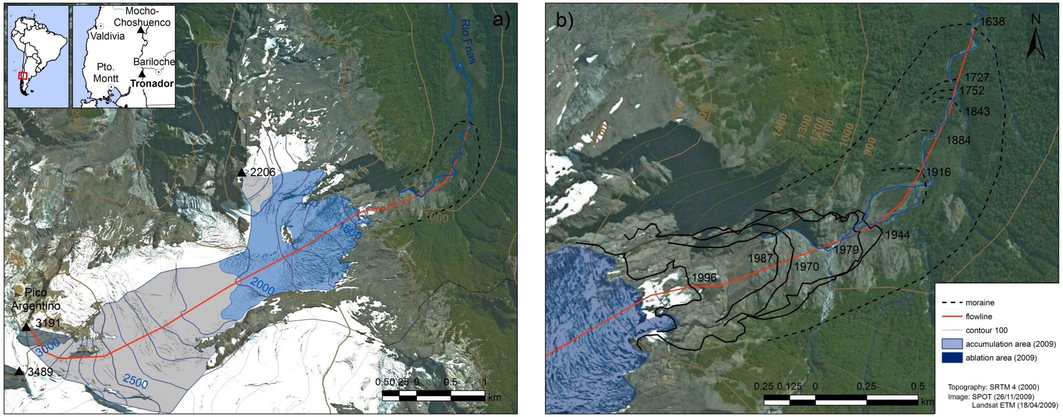

Fig. 1. **(a)** Topography of Glaciar Frías, flowing from the Argentinean summit on the northern slopes of Monte Tronador. The accumulation and ablation area of Glaciar Frías (2009) are indicated with grey and blue shading, respectively. The central flowline is given in red, and altitude in 100 m contour lines. The location of Monte Tronador is shown in the insets. **(b)** Close-up of the glacier forefield with the observed and reconstructed glacier terminus positions. For clarity, not all observations are included.

CPD
7, 3653–3697, 2011

N Patagonian climate from modelling Glaciar Frías

P. W. Leclercq et al.

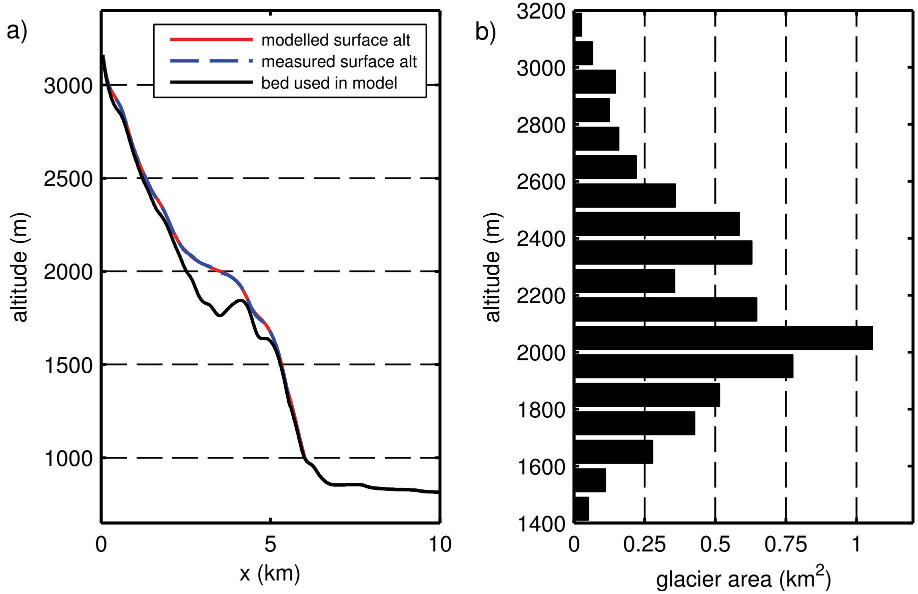

Fig. 2. **(a)** Bed altitude along the glacier flow line (black) from the DEM. For $0 < x < 5.7$ km the DEM gives the ice surface altitude instead of the bed altitude. Here, the bed profile is determined with the ice flow model. The modelled glacier surface (red) differs less than 10 m from the measured surface altitude (dashed blue) (except for $5.7 < x < 6.00$ km, where there is ice in the model run, whereas in 2000 the terminus was at $x \approx 5.7$ km). **(b)** Elevation distribution of the present-day glacier area in 100 m intervals.

CPD
7, 3653–3697, 2011

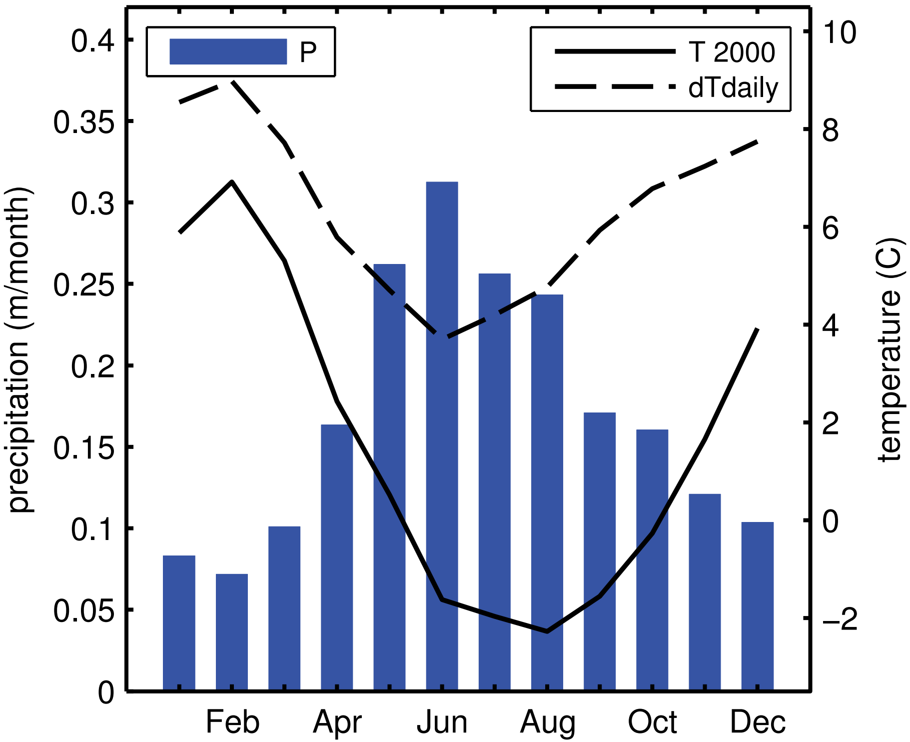

Fig. 3. 1980–2009 climatology of Glaciar Frías, from a combination of ERA-40 and ERA-interim data. Shown are the meteorological parameters needed for the mass balance model: monthly average temperature at 2000 m (black), and amplitude of the daily cycle (dashed black), and average monthly sum of precipitation at 850 m (blue).

CPD
7, 3653–3697, 2011

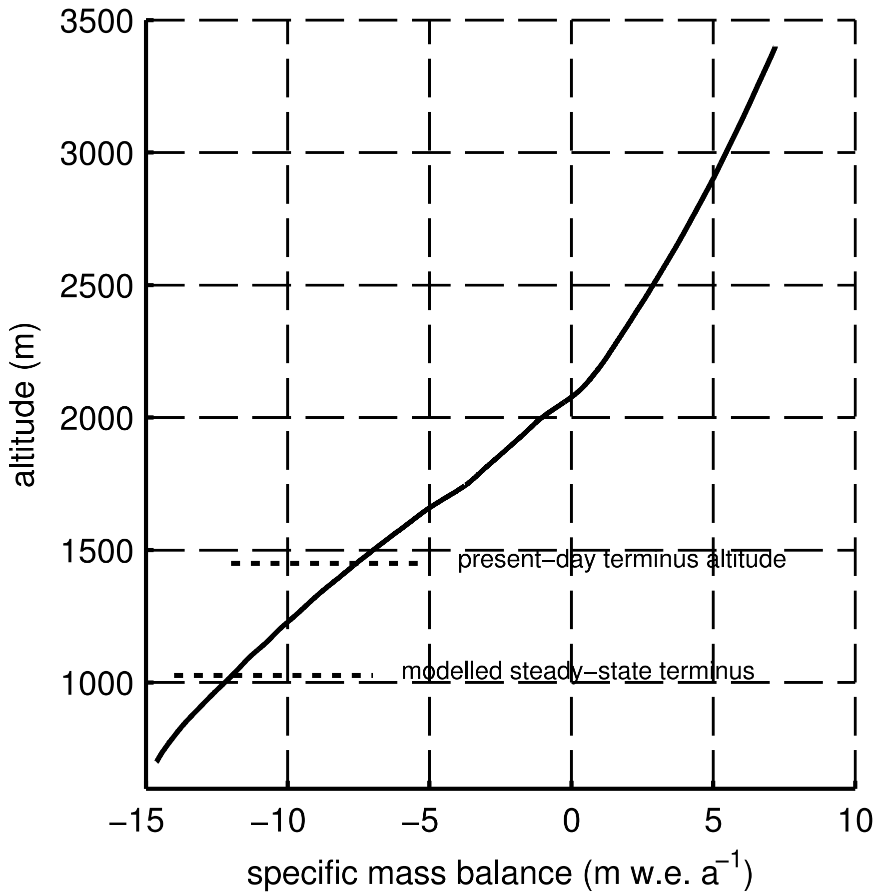

Fig. 4. Mass balance profile $B(z)$ calculated from present-day forcing. NB: the profile is given for the entire model domain, the present-day terminus is at 1450 m (glacier length = 5550 m), the modelled steady-state terminus is at 1027 m altitude (glacier length = 6025 m).

CPD
7, 3653–3697, 2011

N Patagonian climate from modelling Glaciar Frías

P. W. Leclercq et al.

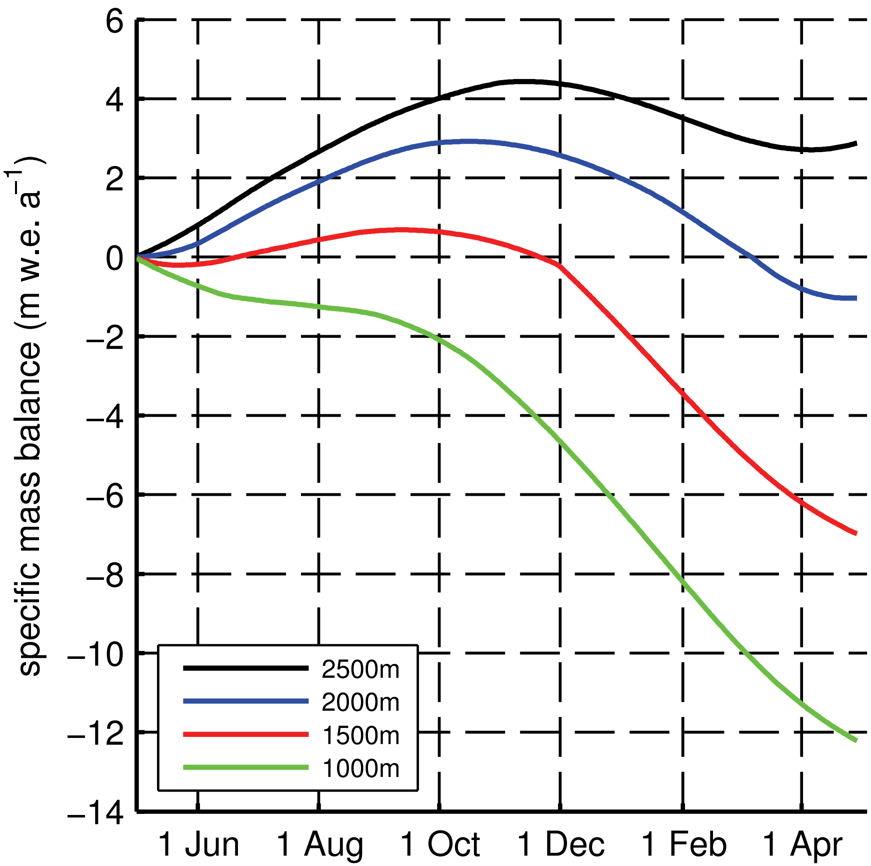

Fig. 5. Temporal evolution of the annual cumulative mass balance, shown in Fig. 4, at selected altitudes. The time evolution is shown during one mass balance year, that starts on 1 May and ends on 30 April.

CPD
7, 3653–3697, 2011

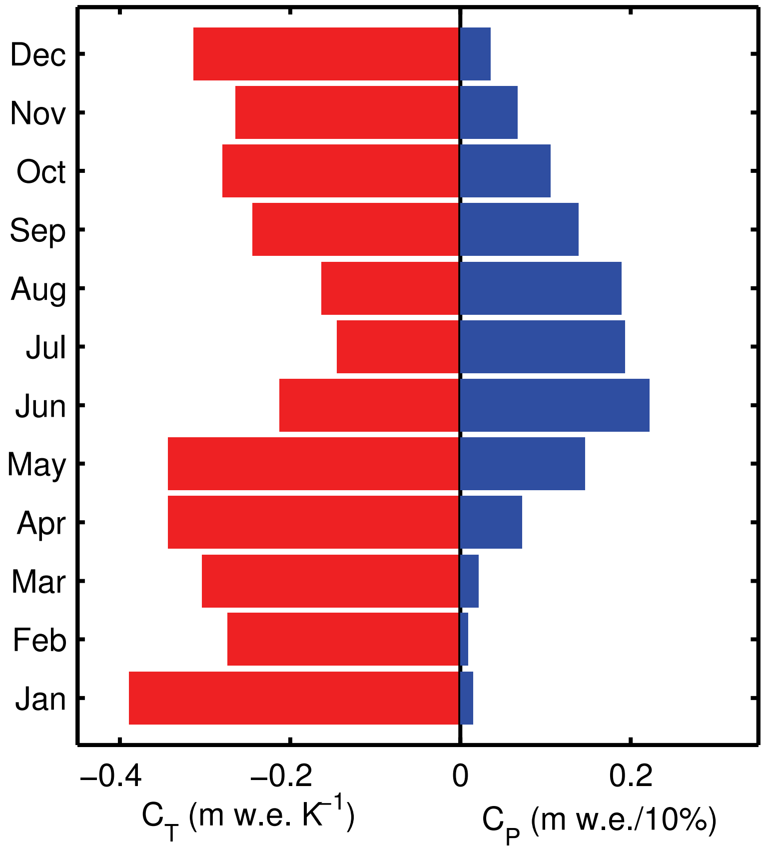

Fig. 6. Seasonal sensitivity characteristic, showing the sensitivity of the mass balance to changes in temperature (C_T) and precipitation (C_P) in a specific month. Changes in precipitation are relative, shown is the change in mass balance after a 10 % change in monthly precipitation. Mass balance is calculated for the glacier geometry of the equilibrium state.

CPD
7, 3653–3697, 2011

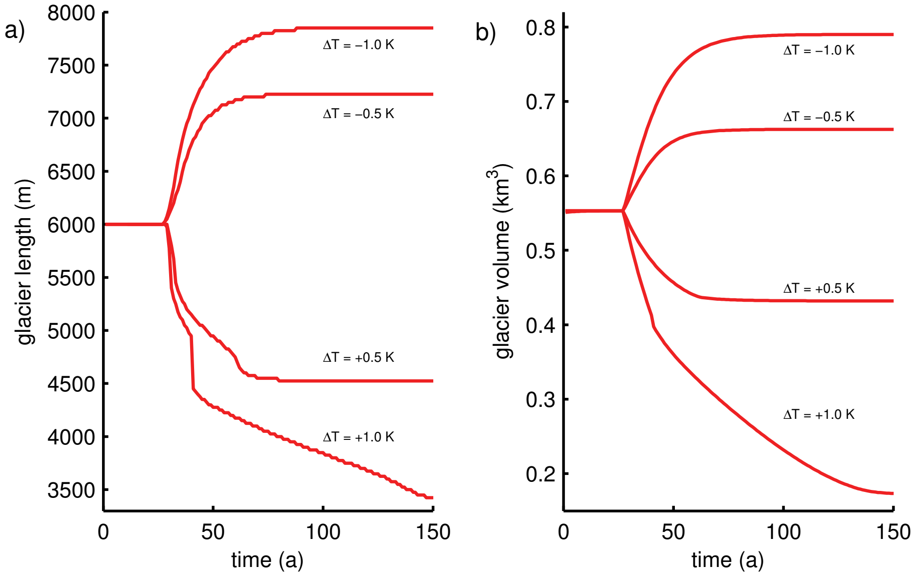

Fig. 7. (a) Length and **(b)** volumes changes of Glaciar Frías after perturbation of the present-day climate with +1.0, +0.5, −0.5 and −1.0 K at $t = 25$ a. It shows the response of Glaciar Frías to perturbations in climate. For $T + 1$ K, the glacier retreats over the overdeepening in the bed, which causes a drastic decrease in both volume and length.

CPD
7, 3653–3697, 2011

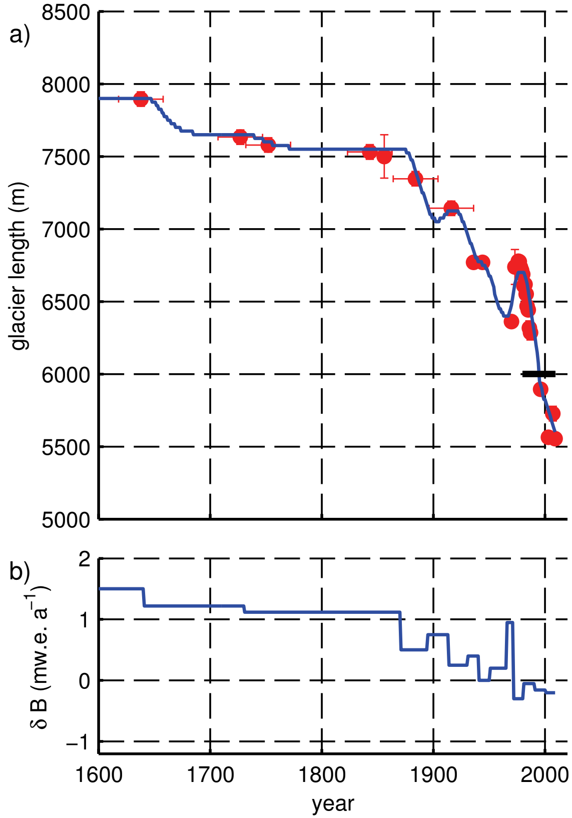

Fig. 8. **(a)** Measured glacier length of Frías (red dots) with bars indicating the uncertainty in both time (dated moraines) and length (most of the times smaller than the dots); modelled equilibrium length for the 1980–2009 climate (black); and modelled glacier length reconstructed with dynamical calibration (blue). **(b)** Mass balance perturbations δB that reproduce the observed glacier length.

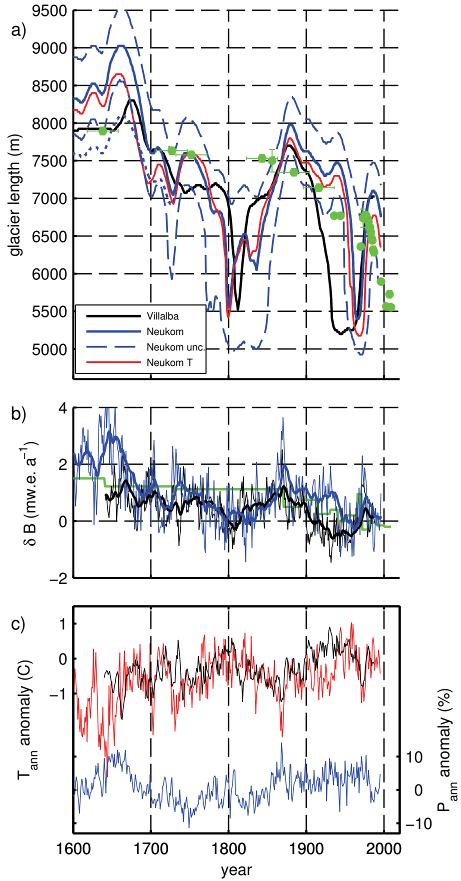

Fig. 9. Caption on next page.

Fig. 9. Results of model forced with the available precipitation (Neukom et al., 2010) and temperature (Neukom et al., 2011; Villalba et al., 2003) reconstructions. **(a)** Glacier length for the period 1600–1995 based on: Neukom et al. (2011, 2010) (blue), with upper and lower estimate (dashed blue) indicating the uncertainty, and the DJF anomaly only applied to summer half year prior to 1706, keeping winter temperatures at 1980–2009 average (blue dotted); Villalba et al. (2003) temperature, Neukom et al. (2010) precipitation (black); Neukom et al. (2011) temperature, precipitation kept constant at the 1980–2009 reference (red); observations (green dots), with uncertainty intervals. **(b)** δB calculated from the annual mass-balance profiles from the reconstructions by Neukom et al. (blue), Villalba et al. (black), with 21-year exponential smoothing, and δB obtained from dynamical calibration (green) (cf. Fig. 8). **(c)** Annual mean temperature anomaly of Neukom et al. (2011) (red) and Villalba et al. (2003) (black) w.r.t. 1980–2009 mean, and annual mean precipitation anomaly of Neukom et al. (2010) w.r.t. the 1600–1995 mean (blue).

CPD
7, 3653–3697, 2011

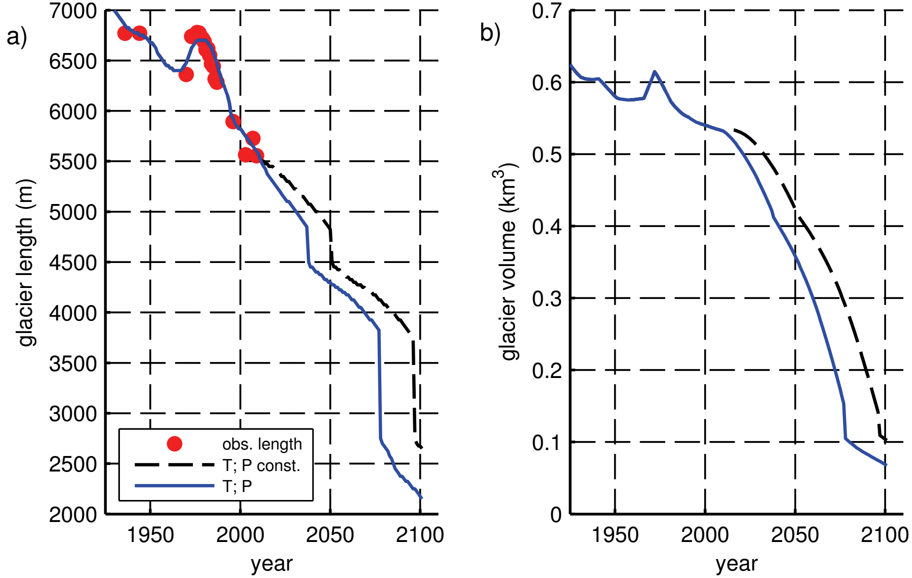

Fig. 10. Modelled **(a)** glacier length and **(b)** glacier volume of Glaciar Frías for the period 1925–2100. Glacier length and volume for the period 1925–2009 are calculated from the reconstructed mass balance profiles, for 2010–2100 the mass balance is calculated from the future scenario. The full scenario (increase in T of 2 °C and decrease in P of 10 % over the 21th century) is shown in blue. The length and volume change with precipitation kept at the 1980–2009 level is given in dashed black. In **(a)** also glacier length observations are included (red dots).

CPD
7, 3653–3697, 2011

N Patagonian climate from modelling Glaciar Frías

P. W. Leclercq et al.